Chapter 2 : Synthesis and Characterization Techniques

2.1 Overview

Chapter 2 provides a comprehensive overview of the materials, synthesis techniques, characterization methods, and software tools employed in the research work. **Section 2.3** outlines an overview of the various synthesis methods employed, including solid-state reaction, sol-gel combustion, and hydrothermal synthesis. These techniques were selected for their ability to precisely control key material properties such as particle size, crystallinity, and doping efficiency. The solid-state reaction is valued for its robustness and scalability, while sol-gel combustion enables the production of fine, homogeneous powders with controlled morphology. The hydrothermal method, by contrast, provides superior control over both the crystallinity and morphology of the resulting materials. Subsequent to the synthesis processes, **Section 2.4** outlines the characterization techniques employed to examine the structural and optical properties of the materials. Techniques including X-ray diffraction (XRD) for phase identification, scanning electron microscopy (SEM) and transmission electron microscopy (TEM) for morphological analysis, energy-dispersive X-ray spectroscopy (EDAX) for elemental composition, Fourier-transform infrared (FTIR) spectroscopy for vibrational analysis, as well as UV-Vis spectroscopy, photoluminescence (PL), upconversion, and decay spectroscopy for optical characterization, are employed. Additionally, other techniques may be utilized depending on the specific properties under investigation, all of which provide valuable insights into the structural and compositional attributes that govern luminescence behaviour. The chapter concludes with Section 2.5, which highlights the software tools employed for data analysis and interpretation, including OriginPro for processing and Full-Proof for visualizing crystal structures. These tools collectively enable a thorough analysis of

the experimental data. In summary, Chapter 2 establishes the experimental groundwork, outlining the methodologies that underpin the findings and discussions in the subsequent chapters.

2.2 Materials Used

This study on lanthanide-doped optical materials utilized a range of high-purity chemicals, to synthesize and investigate various doped versions of calcium molybdate. These materials were carefully selected to ensure efficient dopant incorporation and the achievement of desired optical properties. The detailed specifications of the materials used, including their chemical names, formulas, purities, and manufacturers, are listed in Table 2.1.

Table 2.1 Specifications of Materials Used in Synthesis, Including Chemical Names, Formulas, Purities, and Manufacturers.

S.No	Chemical Name	Formula	Purity (%)	Manufacturer
1	Calcium Oxide	CaO	97	Alfa Aesar
2	Calcium Nitrate Tetrahydrate	$Ca(NO_3)_2 \cdot 4H_2O$	98	Qualigens
3	Molybdenum Trioxide	MoO_3	99.5	Otto Kemi
4	Ammonium Molybdate Tetrahydrate	$(NH_4)_6Mo_7O_{24} \cdot 4H_2O$	99.0	AR grade
5	Erbium (III) Oxide	Er_2O_3	99.9	Alfa Aesar
6	Ytterbium (III) Oxide	Yb_2O_3	99.99	Alfa Aesar
7	Bismuth (III) Oxide	Bi_2O_3	99.99	Alfa Aesar
8	Holmium (III) Oxide	Ho_2O_3	99.9	Alfa Aesar
9	Thulium (III) Oxide	Tm_2O_3	99.99	Alfa Aesar
10	Urea	NH_2CONH_2	-	Fisher Scientific
11	Nitric Acid	HNO_3	69	Merck
12	Propane-2-ol	$(CH_3)_2CHOH$	99.0	Thermo Fisher Scientific
13	Acetone	CH_3COCH_3	99.0	Merck
14	Ethanol	C_2H_5OH	99.9	Changshu Song Sheng

2.3 Synthesis Techniques

Several methods, including the solid-state reaction, hydrothermal, co-precipitation, thermal decomposition, and sol-gel techniques, are commonly employed to synthesize inorganic phosphors. This research employs three distinct synthesis methods to prepare

lanthanide-doped calcium molybdate ($CaMoO_4$) phosphors: the solid-state reaction, sol-gel combustion, and hydrothermal methods, as described in Sections 2.3.1, 2.3.2, and 2.3.3, respectively. Each method was carefully selected to meet specific requirements for doping, crystal formation, and the desired material properties. The solid-state reaction method was employed to synthesize bulk phosphors, while the solution combustion and hydrothermal methods were used for the synthesis of nanophosphors (NPs). The following sections provide an in-depth description of each synthesis method and the phosphor materials produced.

2.3.1 Solid State Reaction Method

The solid-state reaction technique is a widely employed method for synthesizing both pristine and lanthanide (Ln)-doped materials due to its simplicity, scalability, and ability to produce high-purity crystalline compounds. This method involves the reaction of solid-phase precursors, typically high-purity metal oxides, carbonates, or nitrates, which are measured according to stoichiometric calculations and then ground into a homogeneous mixture using ethanol or acetone as a mixing agent. The mixture is then transferred to an alumina crucible and subjected to heat treatment in an electric furnace for thermal treatment. A muffle or box furnace is commonly employed, providing uniform heat distribution and precise temperature control essential for achieving high-quality materials. High temperatures (≥1000°C) are commonly used as it promote diffusion processes, enabling cations or anions to occupy different crystallite sites, which aids in phase formation and ensures uniform doping. The temperature for heat treatment is often determined by Tamman's rule, which suggests that the heating temperature should be approximately two-thirds of the melting point of the constituent compounds. The duration of heat treatment can vary from five to ten hours, or even exceed twenty-four hours, depending on the material being synthesized. During the reaction, gases

such as CO_2, NO_2, NH_3, and O_2 may be released, potentially introducing defects into the material. The procedural schematic for the solid-state synthesis, including the mixing of precursor powders, calcination, and post-synthesis grinding to achieve uniform particle distribution, is shown in Fig. 2.1. The solid-state method is particularly effective for doping lanthanide ions into host materials, as it allows for precise control over doping concentrations and results in luminescent materials with enhanced optical properties, making it ideal for the production of both bulk and doped phosphor materials. The solid-state reaction process consists of four key steps: transport of reactants to the reaction region, diffusion of ions, formation of the new phase, and particle growth. The solid-state method is particularly effective for the incorporation of lanthanide ions into the host lattice, allowing for precise control over doping levels and resulting in phosphors with enhanced optical properties.

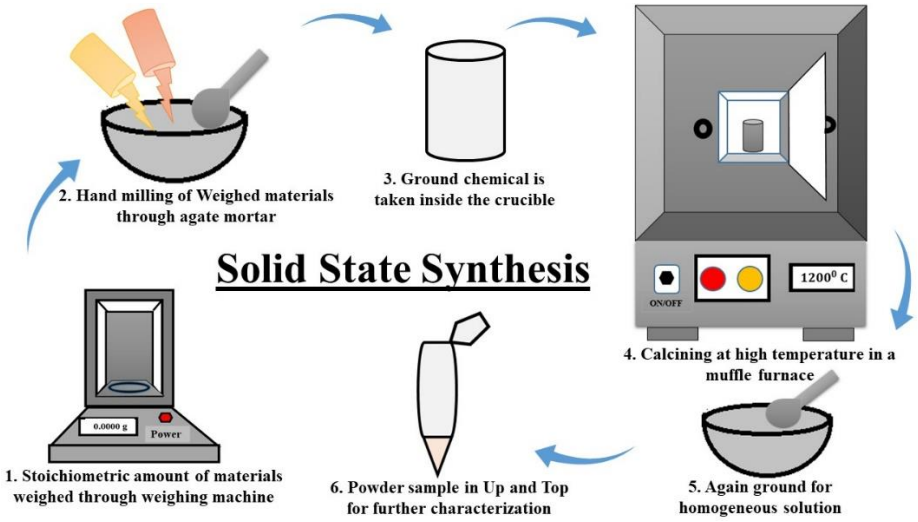

Figure 2.1 Solid-state synthesis procedure for sample preparation, including mixing of precursor powders, calcination in furnace, and post-synthesis grinding to achieve uniform particle distribution.

2.3.1.1 *Synthesis of Pristine $CaMoO_4$ and Er^{3+}/Yb^{3+} Co-Doped $CaMoO_4$*

The synthesis of pristine $CaMoO_4$ and Er^{3+}/Yb^{3+} co-doped $CaMoO_4$ was carried out using the solid-state reaction technique. For this, stoichiometric amounts of precursor powders, including calcium oxide (CaO), erbium oxide (Er_2O_3), ytterbium oxide (Yb_2O_3), and

ammonium molybdate ($AMoO_4$), were carefully measured and mixed. The mixing process was performed thoroughly for 2 hours using a mortar and pestle to ensure a homogeneous distribution of the components. After mixing, the resulting powder was transferred to an alumina crucible and subjected to calcination in a heating furnace at 1200°C for 3 hours. The temperature was increased at a rate of 5°C/min to prevent thermal shock and ensure uniform heating. This calcination step promotes the solid-state reaction, facilitating the formation of $CaMoO_4$ and the incorporation of Er^{3+}/Yb^{3+} ions into the crystal lattice.

Following the calcination, the synthesized materials were cooled and ground into fine, homogeneous powders using an agate mortar and pestle. This grinding process ensured the achievement of a uniform particle size distribution, which is crucial for subsequent applications. The resulting powders were then characterized for structural and optical properties to confirm the successful synthesis of both pristine and co-doped $CaMoO_4$.

2.3.2 Sol-Gel Combustion Method

The sol-gel combustion method is an efficient and adaptable technique for synthesizing phosphor materials, particularly lanthanide-doped phosphors, at significantly lower temperatures than conventional solid-state methods. This approach involves converting a sol (a colloidal solution) into a gel, which then undergoes heat treatment to become a solid. This method facilitates the formation of the final material by combining the advantages of sol-gel processing, such as precise control over chemical composition, particle size, and morphology, with the exothermic nature of the combustion reaction. It is particularly beneficial for the synthesis of oxide-based materials, allowing for tight control over the final product's characteristics.

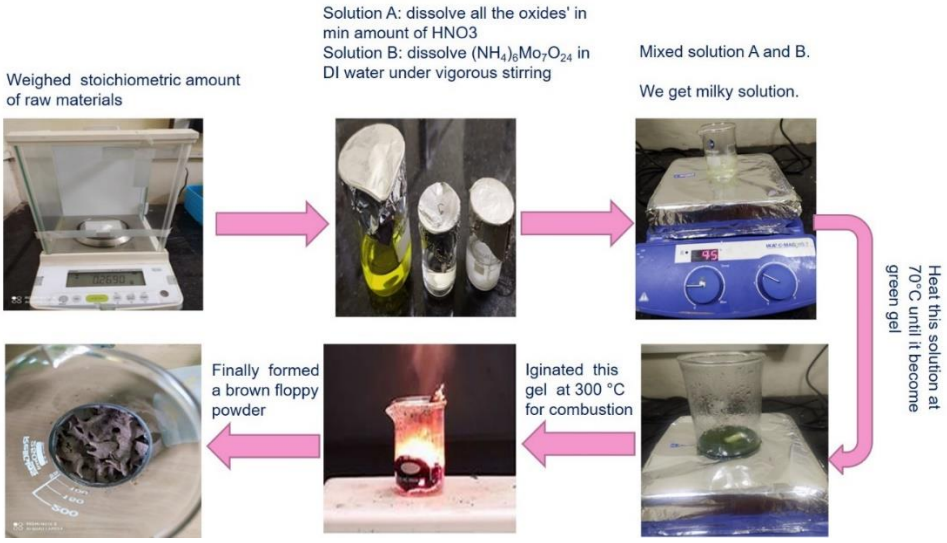

Figure 2.2 Sol-gel synthesis procedure for sample preparation, including sol formation, gelation, thermal decomposition (combustion), and post-synthesis grinding for uniform particle distribution.

The process begins by mixing precursor nitrates with a fuel, such as urea, glycine, or citric acid. These mixtures form a transparent gel, which is then placed in a platinum crucible and subjected to heat in a preheated furnace, typically maintained at temperatures between 450°C and 550°C. The exothermic combustion reaction is triggered as the gel melts and undergoes thermal decomposition, releasing ammonia and nitrogen oxides as brown fumes. The result is the formation of a foamy, whitish material. This combustion process lasts around 5 to 10 minutes, after which the foam is cooled and solidified. The cooled product is crushed into a fine powder using an agate mortar and may undergo further heat treatment to refine its structure. A schematic representation of the Sol-gel synthesis technique is provided in Fig 2.2.

The fuel plays a pivotal role in the sol-gel combustion method, influencing the formation of complex oxide compounds and ensuring uniform particle size distribution. The fuel employed in this method, such as urea, glycine, or citric acid, plays a crucial role in ensuring uniform particle size distribution and facilitating the formation of complex oxide-based compounds. The combustion process itself can include various types of reactions such

as flaming, smoldering, and explosive combustion, each contributing to the final material's formation. These reactions generate high temperatures, essential for synthesizing oxide materials, particularly those that form complex structures. Overall, the sol-gel combustion method offers several advantages over traditional solid-state synthesis, enabling the production of phosphor materials at lower temperatures with precise control over key properties like morphology and particle size. This is especially important for lanthanide-doped phosphors, where such control directly impacts the material's optical properties, such as emission spectra and quantum efficiency.

2.3.2.1 *Synthesis of Pristine and Er^{3+}/Yb^{3+}, $Er^{3+}/Yb^{3+}/Bi^{3+}$ Co-Doped $CaMoO_4$*

In the synthesis of pristine and Er^{3+}/Yb^{3+}, $Bi^{3+}/Er^{3+}/Yb^{3+}$ co-doped $CaMoO_4$, stoichiometric amounts of key precursors, including calcium oxide (CaO) and dopants such as Er_2O_3, Yb_2O_3, and Bi_2O_3, are mixed with nitric acid (HNO_3) to convert them into their respective metal nitrates. The resulting metal nitrate solution is then washed with deionized water at least twice to remove excess nitric acid. In a separate beaker, 30 mL of deionized water is used to dissolve the prepared metal nitrates, and urea is added as a fuel. Ammonium molybdate, a water-soluble compound, is also used in the process. The mixture is then heated to 85°C for 15 minutes to facilitate the reaction. Once all the nitrate solutions are prepared, they are combined and heated at 200°C with continuous stirring until a gel-like material forms. The gel is then subjected to thermal treatment by heating to 500°C, which triggers auto-ignition and results in the formation of a foam-like ceramic material. This sol-gel process enables the synthesis of $CaMoO_4$ and its doped variants, such as Er^{3+}/Yb^{3+} and $Bi^{3+}/Er^{3+}/Yb^{3+}$

co-doped $CaMoO_4$, with precise control over composition, particle size, and morphology, making it ideal for producing high-quality phosphor materials.

2.3.3 Hydrothermal method

The hydrothermal process is highly relevant in the synthesis of inorganic materials, particularly phosphors, due to its ability to offer precise control over material properties like crystallinity, particle size, and morphology. This method operates under high-temperature and high-pressure conditions, enabling the synthesis of high-purity, defect-free materials that are difficult to obtain through other techniques. Its versatility in producing a wide range of materials, including doped phosphors, makes it an attractive choice for advanced applications such as optoelectronics, luminescent devices, and energy-efficient lighting.

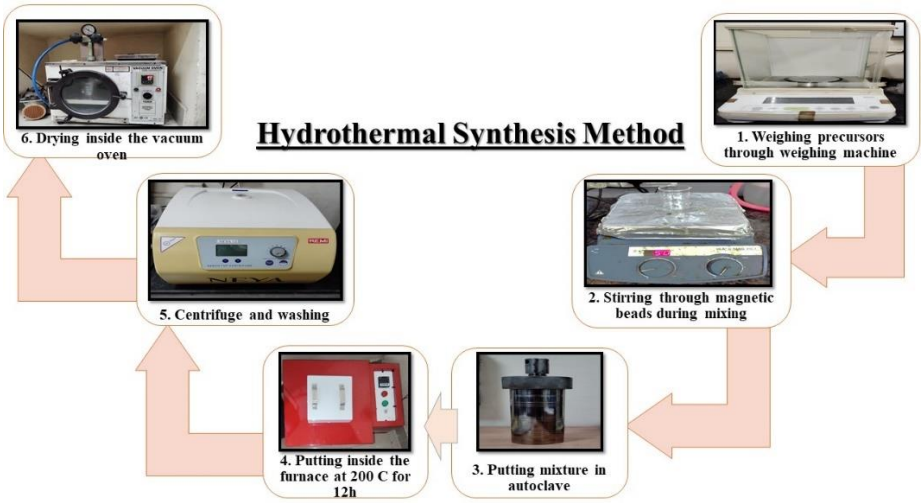

Figure 2.3 Schematic of the hydrothermal synthesis of phosphors, including precursor preparation, autoclave reaction, and post-synthesis cooling, washing, and drying.

In the basic hydrothermal synthesis procedure, metal salts (such as metal nitrates, chlorides, or acetates) are mixed with rare-earth dopants (e.g., Er^{3+}, Yb^{3+}, or Eu^{3+}) in deionized water to form precursor solutions. The precursor mixture is then transferred to a Teflon-lined stainless-steel autoclave, which is sealed and heated to temperatures between 150°C and 250°C under pressures of 5–20 MPa. The high-pressure and high-temperature

conditions facilitate the dissolution of precursors and the formation of crystalline materials, such as phosphors. After the reaction, the product is cooled, filtered, washed with deionized water, and dried. Additional thermal treatment, like annealing, may be performed to enhance material properties. Fig 2.3 illustrates the key steps of the hydrothermal synthesis, including precursor preparation, reaction, washing, and calcination. Compared to other methods like solid-state reactions and sol-gel techniques, the hydrothermal process offers several advantages. It operates at lower temperatures, saving energy and preventing degradation of sensitive materials. It also provides better control over particle size and dopant distribution, resulting in high-quality, homogeneous materials. Furthermore, the ability to produce nanoscale particles enhances the luminescent properties of phosphors, making it a superior choice for high-performance materials.

2.3.3.1 *Synthesis of Pristine and $Tm^{3+}/Ho^{3+}/Yb^{3+}$ co-Doped $CaMoO_4$*

The synthesis of $Tm^{3+}/Ho^{3+}/Yb^{3+}$ co-doped $CaMoO_4$ was achieved through a hydrothermal process followed by post-calcination to enhance the material's crystallinity. The precursor materials, including calcium nitrate tetrahydrate ($Ca(NO_3)_2 \cdot 4H_2O$) and ammonium molybdate, which readily dissolve in water, were used alongside the lanthanide dopants, such as Holmium oxide (Ho_2O_3), Thulium oxide (Tm_2O_3), and Ytterbium oxide (Yb_2O_3). These lanthanide oxides were initially dissolved in dilute nitric acid (HNO_3) at 80°C to form their corresponding nitrates. A 5 mL aqueous solution of these lanthanide nitrates was then prepared and mixed with preheated deionized water at 80°C, with continuous stirring for 2 hours to ensure complete dissolution. Following the preparation of the precursor solution, it was transferred into a Teflon-lined stainless-steel autoclave, where the hydrothermal reaction took place at 140°C for 24 hours. This reaction resulted in the formation of the desired

phosphor material. After cooling the autoclave to room temperature, the phosphor samples were subjected to 2-3 wash cycles using ethanol and water via centrifugation to remove any residual impurities. The washed samples were then dried and calcined at 750°C to further enhance their crystallinity and optimize their optical properties. The hydrothermal method, followed by calcination, ensures uniform dopant distribution and controlled material structure, significantly improving the optical performance of the resulting phosphor.

2.4 Instrumentation used in present thesis

The characterization of synthesized phosphor materials is crucial for understanding their properties, and this section outlines the techniques used for the structural, optical, and morphological analysis of lanthanide-doped $CaMoO_4$-based phosphors. After preparing the inorganic phosphor samples, advanced instrumentation was employed to investigate their structural, optical, and magnetic properties. The rapid advancements in instrumentation technology have significantly enhanced material research, enabling comprehensive analysis across multiple domains. For structural characterization, X-ray diffraction (XRD) was used, while morphological properties were examined using field emission scanning electron microscopy (FE-SEM) and transmission electron microscopy (TEM). Optical properties were studied using a range of techniques, including photoluminescence (PL) spectroscopy, UV–visible-near infrared (NIR) spectroscopy, Fourier transform infrared (FTIR) spectroscopy, Raman spectroscopy, and decay lifetime measurements. Additionally, advanced instruments such as the up-conversion emission spectrometer were utilized to gain deeper insights into the material's properties.

2.4.1 X-ray Diffraction (XRD)

X-ray diffraction (XRD) is a powerful technique used for the phase analysis of materials, providing essential information about the crystalline structure, phase composition, and lattice parameters of synthesized phosphor materials. By measuring the diffraction pattern produced when X-rays interact with the crystalline sample, XRD helps identify the phases present in the material and determine their crystallographic details. It is particularly useful for confirming the formation of the desired phase of inorganic phosphors and also for detecting any impurity phases. In addition to phase identification, XRD can provide insights into other important properties, such as crystallite size, strain, phase composition and the degree of crystallinity. These structural insights are fundamental for correlating the material's properties with its performance in optical and other functional applications.

2.4.1.1 *Basic principle*

X-ray diffraction (XRD) is a key technique for analysing the crystal structures of materials, whether single crystals or polycrystalline substances. X-rays, discovered by W.C. Röntgen in 1895, are electromagnetic radiation with wavelengths typically between 0.7 and 2 Å, allowing them to penetrate solid materials and offer detailed insights into their internal crystalline structures. The XRD technique is rely on Bragg's Law, formulated by Sir William Henry Bragg and William Lawrence Bragg in 1915, which connects the diffraction angle (θ) to the spacing between atomic planes in the crystal lattice (d) and the wavelength of the X-rays (λ). Bragg's Law is expressed as:

$$2d\mathrm{Sin}\theta = n\lambda \qquad \ldots (2.1)$$

where *n* is the diffraction order, λ is the X-ray wavelength, d is the plane spacing, and θ is the diffraction angle. When X-rays interact with the crystal lattice, constructive interference occurs, producing distinct diffraction peaks. These peaks provide valuable information about the material's atomic arrangement, interatomic distances, and crystalline phases, making XRD an essential tool for studying polycrystalline materials.

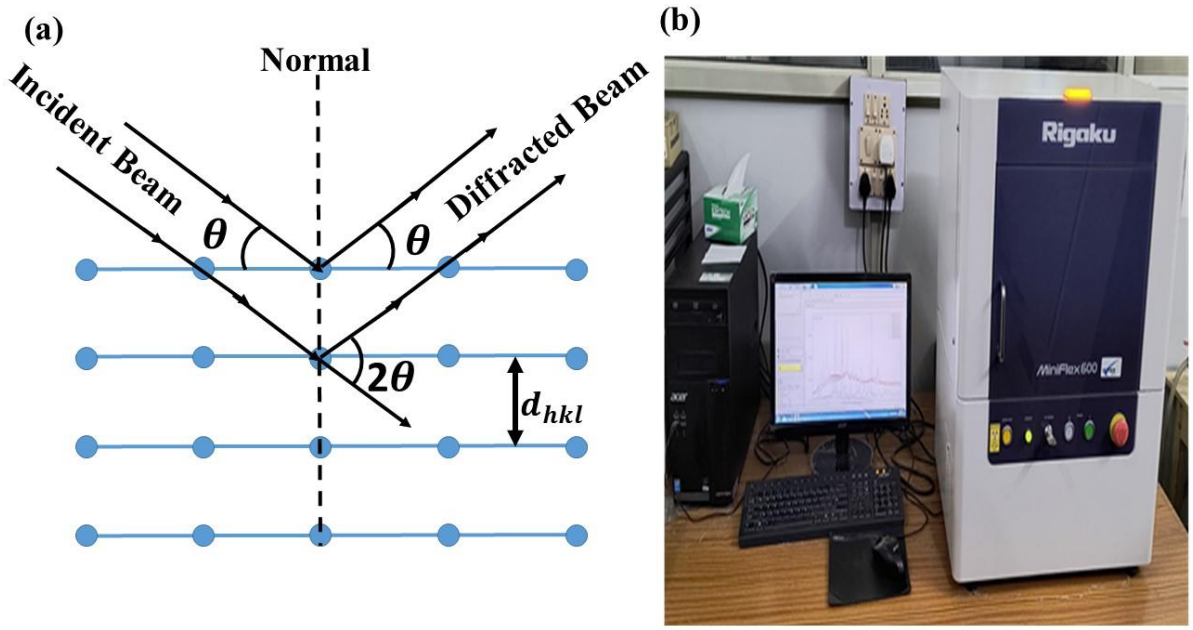

Figure 2.4 ***(a)*** *Illustrates the fundamental mechanism of X-ray diffraction, where incident X-rays are reflected off consecutive lattice planes, generating interference patterns unique to each material.* ***(b)*** *X-ray diffractometer (MiniFlex 600, Rigaku, Japan), CIF IIT (BHU).*

In this thesis, XRD data were collected using a MiniFlex 600 diffractometer (Rigaku, Japan) equipped with Cu Kα radiation (λ=1.5406 A˚), as shown in Fig. 2.4. The diffractometer operated at 40 kV and 15 mA, scanning over a 2θ range of 10° to 90° with a step size of 0.02° and a scanning rate of 5°/min. The diffraction peak positions and intensities were compared with the Joint Committee on Powder Diffraction Standards (JCPDS) database to assess the crystallinity and phase purity of developed materials (herein $CaMoO_4$) samples. Additionally, the XRD patterns were cross-verified using the ICDD (International Center for Diffraction

Data) database, which provides a comprehensive collection of diffraction patterns for a wide range of materials.

2.4.1.2 *Crystalline size and Lattice parameters calculation:*

Calculating crystallite size and lattice parameters from XRD data is essential for understanding the structural properties of synthesized materials. The crystallite size (D) of the synthesized phosphors was estimated using the Debye-Scherrer equation:

$$D = \frac{K\lambda}{\beta \cos\theta_B} \qquad \ldots (2.2)$$

where K is a constant (typically 0.9), λ is the X-ray wavelength, β is the full width at half maximum (FWHM) of a diffraction peak, and θ_B is the Bragg angle. This equation is valid for particles smaller than 100 nm, which applies to the synthesized samples. It is important to distinguish between crystallite size, which refers to the coherent scattering domain with a perfect crystal structure, and grain or crystal size, which may include multiple crystallites or regions with defects. When particle size exceeds 100 nm, lattice strain becomes significant, making the William-Hall (W-H) plot a more relevant method. Unlike the Debye-Scherrer method, which primarily estimates crystallite size, the W-H plot directly accounts for both crystallite size and strain by analysing peak broadening through a linear plot of $\beta\cos\theta$ versus $\sin\theta$, allowing separation of size and strain contributions. In addition to crystallite size, lattice parameters (a, b, c) and angles (α, β, γ) of the doped $CaMoO_4$ were calculated using unit cell refinement software such as FullProf. The Rietveld refinement method in FullProf provides precise values for these parameters, offering insights into atomic positioning within the unit cell. The sharpness of XRD peaks indicates a high degree of crystallinity, which supports the structural integrity of the material, even after doping with lanthanides. These measurements are crucial for correlating the material's structure with its optical and functional properties.

2.4.2 Morphological Analysis

Morphological analysis is crucial for elucidating the surface features, particle size, and shape of phosphor materials. This study utilized SEM and HR-TEM to examine the surface morphology and particle distribution. Electron microscopy, with its high resolution, is ideal for studying nanoparticles' size, shape, and structure, as it overcomes the diffraction barrier that limits optical microscopes. Unlike optical microscopy, electron microscopes use electron waves, which have much shorter wavelengths, enabling finer resolution. The SEM and TEM techniques employed in this research facilitated detailed analysis of nanoparticle or microparticles morphology, size distribution, and surface characteristics, providing valuable insights into the structural properties and behaviour of the phosphor materials.

2.4.2.1 *Scanning Electron Microscopy (SEM)*

Scanning Electron Microscopy (SEM) is a crucial technique in materials science for analysing surface morphology, particle size, and elemental composition. It works by scanning the sample surface with a focused beam of high-energy electrons, which generate secondary and backscattered electrons. These electrons are detected to produce high-resolution images. The resolution of SEM images depends on the size of the electron beam spot, typically around ~5 nm, and the energy range of the beam, which can vary from few hundred eV to 50 keV. In this study, SEM analysis was performed using an EVO Scanning Electron Microscope MA15/18 (CARL ZEISS MICROSCOPY LTD), operating at 20 kV. Phosphor samples were coated with a thin gold layer to prevent charging effects, allowing for clearer imaging. Images were captured at various magnifications using an Everhart-Thornley detector, which collects both secondary and backscattered electrons, providing topographic contrast and some elemental composition details. The resulting images enabled detailed analysis of the textures

of the phosphor particles, including features like agglomeration and porosity, and allowed for estimating particle dimensions. Apart from this, FE-SEM is an advanced version of SEM, offering higher resolution and contrast, especially for non-conductive materials. Unlike traditional thermionic emitters (tungsten or LaB_6), FE-SEM uses a field emission electron gun that operates at lower voltages. This minimizes charging effects on non-conductive samples, enabling clearer, higher-magnification images. FE-SEM also features condenser and objective lenses to focus the electron beam, along with apertures to control its size. Magnetic scan coils ensure precise alignment for point-by-point scanning of the specimen (ray-diagram in Fig. 2.5 (a).

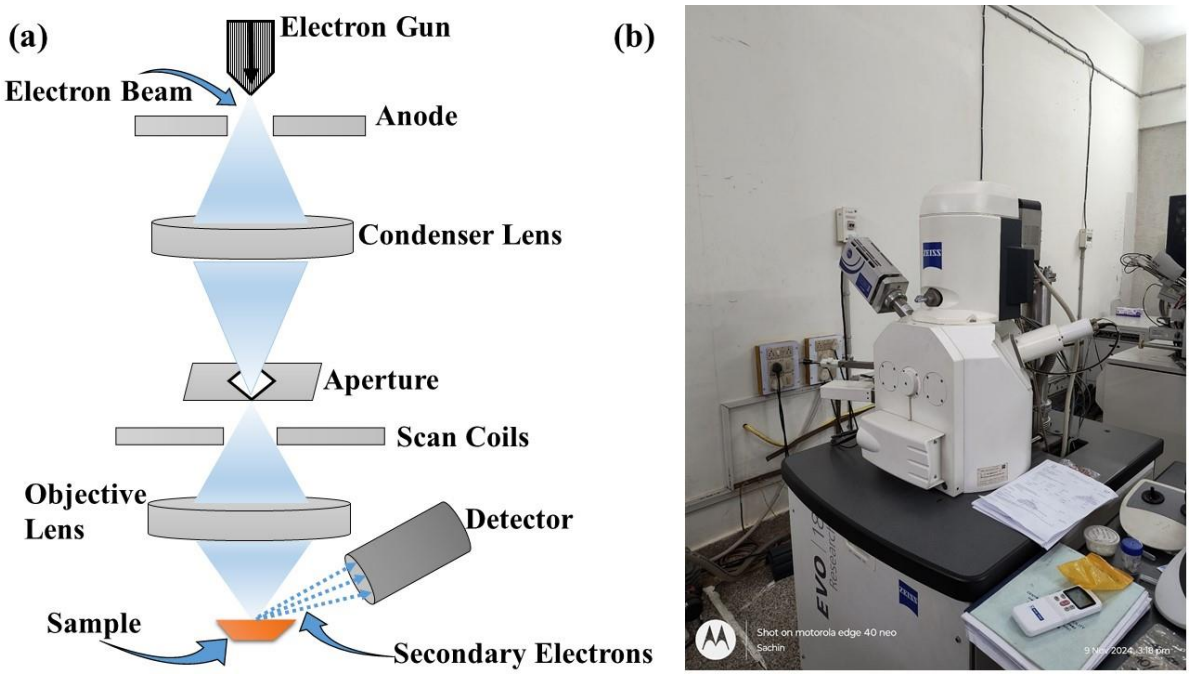

Figure 2.5 ***(a)*** *Schematic diagram of the instrumental set up of Field emission scanning electron microscope (FE-SEM).* ***(b)*** *Digital photograph of the EVO – SEM MA15 / 18, CARL ZEISS (CIF, IIT BHU).*

Energy Dispersive X-ray analysis spectroscopy (EDAX) was used in conjunction with SEM to perform compositional analysis using the 51N1000 EDS system (Oxford Instruments Nano Analysis). EDX enables the detection of characteristic X-rays emitted by the sample when bombarded by an electron beam, allowing for detailed, quantitative analysis of

elemental composition. This technique confirmed the presence of elements such as Ca, Mo, O, as well as dopant ions like Er^{3+}, Yb^{3+}, Tm^{3+}, Ho^{3+}, and Bi^{3+} in the synthesized phosphors. The high-energy electron beam in SEM generates multiple signals, including secondary electrons (SE), backscattered electrons (BSE), and Auger electrons. While SE and BSE primarily provide topographic contrast and insight into elemental composition, Auger electrons contribute additional chemical composition details. These signals are collected by specialized detectors, converted into photons, amplified by photomultiplier tubes, and then transformed into electrical signals to produce a comprehensive image of the sample.

2.4.2.2 *High-Resolution Transmission Electron Microscopy (HR-TEM)*

High-Resolution Transmission Electron Microscopy (HR-TEM) is a vital tool for examining the particle size, morphology, crystal structure, and microscopic defects in nanostructured materials. With a resolution often exceeding 2 nm, HR-TEM provides detailed imaging of internal features, making it especially valuable for studying the crystallography of materials. Developed by Max Knoll and Ernst Ruska in 1933, HR-TEM operates similarly to Scanning Electron Microscopy (SEM), but with higher magnification and finer resolution. While SEM focuses on surface analysis, HR-TEM transmits an electron beam through an ultra-thin sample to generate detailed images of its internal structure. In this study, HR-TEM analysis was conducted using a Tecnai G2 20 TWIN microscope (FEI Company), as shown in Fig. 2.6 (a). Phosphor samples were finely ground, dispersed in ethanol, and drop-cast onto a carbon-coated copper grid, which is a common and stable mount for TEM imaging. The grid was vacuum-dried to ensure high-quality imaging. HR-TEM imaging provided insights into the crystal structure, size distribution, and agglomeration behaviour of lanthanide-doped $CaMoO_4$ phosphor particles.

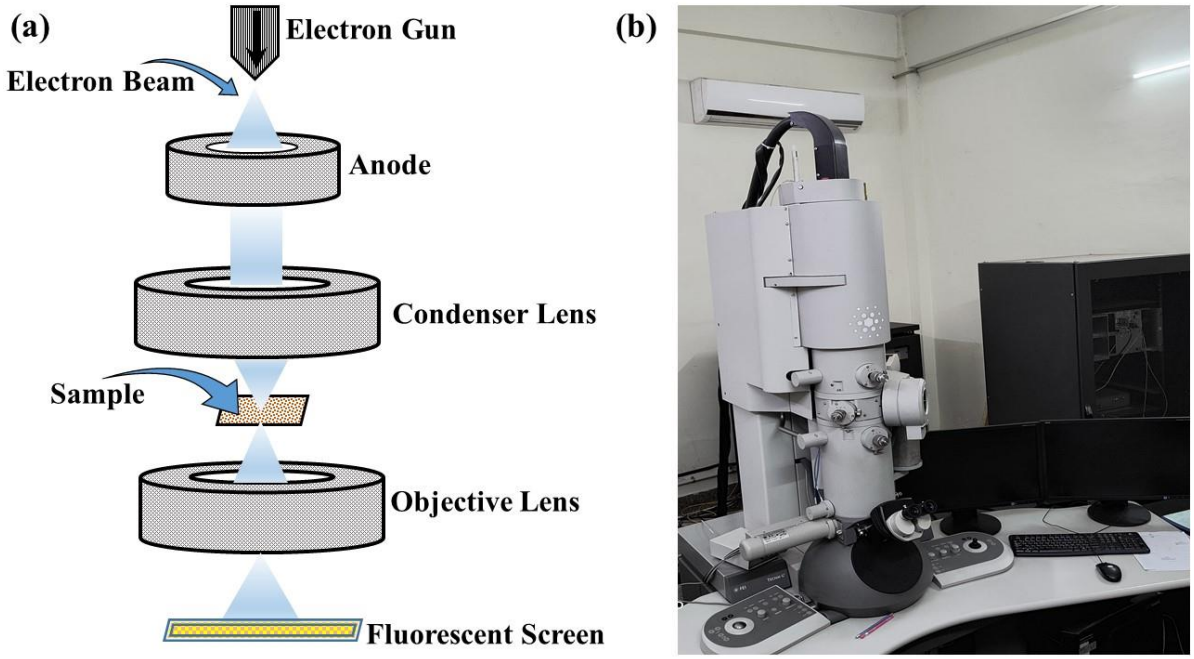

Figure 2.6 (a) Schematic diagram of instrumental set up of Transmission Electron Microscopy (TEM). (b) Digital photograph of Tecnai G2 20 TWIN, HR-TEM setup (CIF IIT BHU).

The TEM setup includes key components such as an electron source (electron gun), electromagnetic lenses, condenser aperture, objective lens, sample stage, image recording system, and detector, all arranged to focus and direct the electron beam as shown in Fig. 2.6 (b). The high accelerating voltage (100–300 kV) produces shorter electron wavelengths, enabling high-resolution imaging. The transmitted electrons form an image on a fluorescent screen, revealing the sample's internal features. For crystallinity analysis, Selected Area Electron Diffraction (SAED) patterns were obtained using an Octane Plus SDD detector (EDAX Inc.), providing detailed information on the atomic arrangement within the phosphor particles. In conclusion, TEM provides both imaging and diffraction analysis, allowing for a thorough assessment of the morphological and structural properties of the synthesized phosphors.

2.4.3 Spectroscopic Methods for Material Characterization

Spectroscopic characterization is essential for understanding and enhancing phosphor materials, typically categorized into vibrational and optical spectroscopy. These techniques provide valuable insights into the chemical, structural, and optical properties of phosphors by analysing their interactions with different types of radiation. These methods are essential for assessing key factors such as energy transfer mechanisms, luminescent efficiency, the impact of crystal defects, doping effects, and the overall material performance under different conditions. Vibrational spectroscopy techniques, such as Fourier Transform Infrared (FTIR) and Raman spectroscopy, are essential for investigating the molecular vibrations and bonding characteristics within phosphor materials. FTIR is effective in identifying functional groups and bonding types, while Raman spectroscopy offers insights into lattice vibrations, crystal symmetry, and structural defects. Both methods are valuable for understanding how the material's molecular and crystalline structure affects its luminescent behaviour. Conversely, optical spectroscopy techniques play a crucial role in examining the light emission properties of phosphors. UV-Vis spectroscopy analyses the absorption spectrum, providing information on excitation wavelengths and photon absorption efficiency. Photoluminescence (PL) spectroscopy characterizes the emission spectra, offering insights into the light output and material efficiency. Up-conversion spectroscopy is particularly useful for materials that absorb low-energy photons and emit higher-energy ones. Additionally, decay time measurements are important for evaluating radiative and non-radiative recombination processes. These spectroscopic methods provide a comprehensive understanding of phosphor materials, aiding their optimization for various applications, with detailed discussions provided below.

2.4.3.1 *Fourier-Transformation Infrared (FTIR) Spectroscopy:*

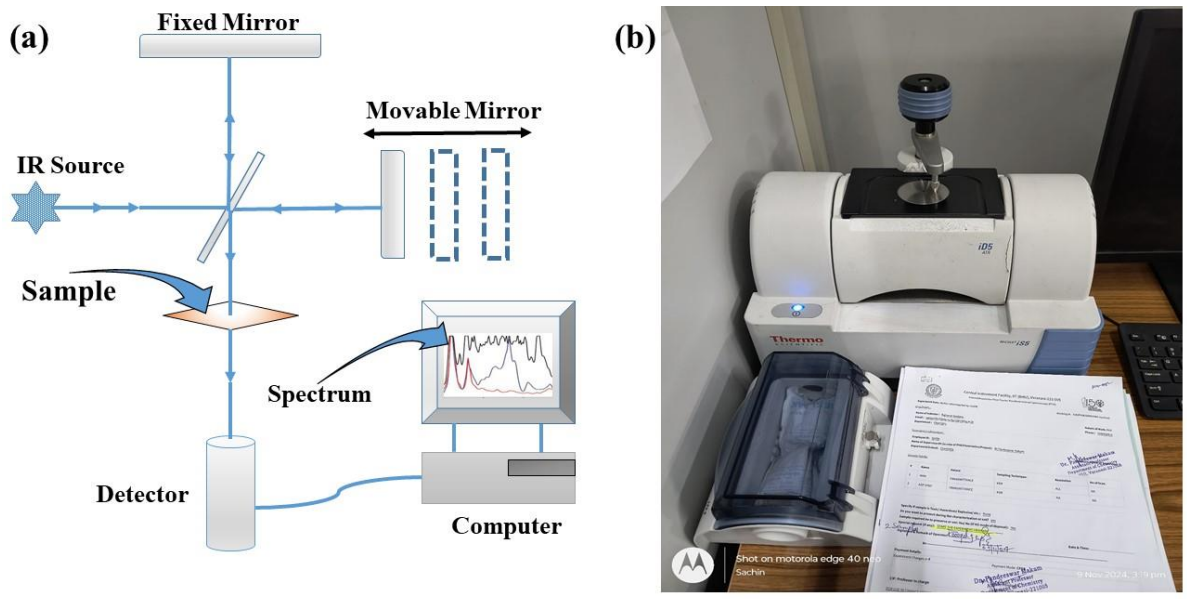

Figure 2.7 (a) Ray diagram of FT-IR spectroscopy. (b) Digital photograph of Nicolet iS5, Thermofisher (CIF, IIT BHU).

FTIR spectroscopy measures the absorption of infrared radiation by a sample, providing insights into its molecular bonds and functional groups. Different type of bonds absorbs infrared radiation at specific frequencies, corresponding to the vibrational motions of covalently bonded molecules. When infrared light interacts with the sample, it undergoes absorption, reflection, scattering, or transmission, revealing information about the chemical bonding. The FTIR spectrometer consists of an IR source, beam splitter, mirrors, sample compartment, and detector. The IR radiation is split into two beams, one reflected and one transmitted, which then interfere to produce an interferogram. This signal is processed via Fourier transformation to generate a spectrum of frequency and intensity. The ray diagram for FTIR spectroscopy is presented in Fig. 2.7 (a). FTIR spectra are recorded in the mid-IR region (400-4000 cm^{-1}) using a Nicolet iS5 spectrometer from Thermo Fisher shown in Fig. 2.7 (b). A Nernst glower, commonly used as the IR source, was utilized due to its efficiency in the

mid-IR range. The system employed thermal detectors such as deuterated tri-glycine sulfate (DTGS) for the mid-IR range and a Si-bolometer for the far-IR region (10-400 cm^{-1}). Photon detectors, including array diode detectors, were used to detect IR radiation based on semiconductor material interaction.

In this thesis, FTIR analysis was employed to identify the vibrational groups corresponding to specific bonds, thereby confirming the formation of $CaMoO_4$ phosphors, particularly by detecting the Mo–O bonds within the MoO_2^{2-} tetrahedral units. It is also useful for detecting unwanted groups, such as moisture or residual reactants like carbonates, nitrates, amines, and others, which can be easily identified in inorganic samples, while organic materials and their corresponding bands are readily distinguishable. In conclusion, FTIR spectroscopy is an effective technique for analysing molecular bonds, verifying the formation of $CaMoO_4$ phosphors, and identifying functional groups as well as unwanted residual group/compounds in samples.

2.4.3.2 *Raman Spectroscopy:*

Raman spectroscopy is a powerful technique that investigates vibrational, rotational, and electronic energy modes in molecules, offering insights into chemical bonds, molecular structure. It also provides information on symmetry, crystallinity, and structural defects through shifts in the Raman spectra. This technique relies on the inelastic scattering of photons, known as Raman scattering, a phenomenon first observed by Sir C. V. Raman in 1922 [9]. When monochromatic light, usually from a laser, interacts with a material, most photons are elastically scattered (Rayleigh scattering). However, a small fraction undergoes inelastic scattering, causing an energy shift that corresponds to the vibrational frequencies of the material's chemical bonds.

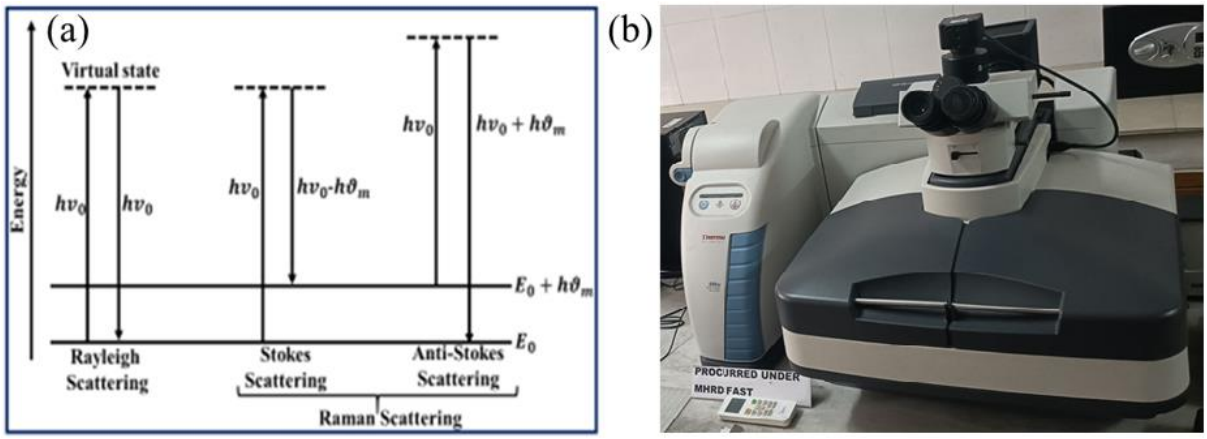

Figure 2.8 ***(a)*** *Possible energy diagrams of Rayleigh and Raman scattering process. (b) Digital photograph of Raman setup DXRxi, Thermo Scientific (Department of Physics, Banasthali Vidyapith, Jaipur).*

Raman scattering is rare, with only about one photon in 10^{12} undergoing inelastic scattering when striking a molecule. This can be mitigated by using a high-power laser, as Raman scattering intensity is proportional to the square of the incident field. Mathematically, if an electric field $E = E_0 cos(w_0 t)$ is applied to a molecule vibrating at an angular frequency ω_m, the resulting Raman intensity I_{RS} can be expressed as:

$$I_{RS} \propto \left(\frac{\partial \alpha}{\partial x} E_o[\cos(w_o - w_m)\, t + \cos(w_o + w_m)t]\right)^2 \quad \ldots (2.5)$$

In this expression, α represents the molecular polarizability, x denotes the nuclear displacement, and ω_0 is the angular frequency of the incident field. It shows that the scattered photons can have energies either lower $\hbar(\omega_0 - \omega_m)$ or higher $\hbar(\omega_0 + \omega_m)$ than the incident photons, corresponding to Stokes and Anti-Stokes scattering, respectively. For a molecule to exhibit Raman activity, there must be a change in polarizability with nuclear displacement, i.e., $\frac{\partial \alpha}{\partial x} \neq 0$. A schematic of the Rayleigh and Raman scattering processes is shown in Fig. 2.8(a).

This study used Raman spectroscopy to examine the vibrational modes of both pristine and Ln-doped $CaMoO_4$ phosphors. The Raman spectra were collected using a DXRxi Raman Imaging Microscope (Thermo Scientific, USA) with a 532 nm laser source, covering the range

of 100–1000 cm^{-1}, as shown in Fig. 2.8(b). The spectra serve as a molecular "fingerprint," with peaks corresponding to the vibrational frequencies of the MoO_4^{2-} tetrahedral units in the $CaMoO_4$ lattice. The spectrum of pure $CaMoO_4$ shows intense peaks from the symmetric stretching and bending of Mo–O bonds, reflecting the fundamental vibrational modes of the tetrahedral units. Doping the $CaMoO_4$ matrix with lanthanides like Er^{3+}, Yb^{3+}, and other rare-earth ions causes shifts in the Raman peaks, indicating structural changes in the local lattice due to dopant incorporation. These ions, differing in size and charge from the host cations, induce lattice distortions that affect the MoO_4^{2-} vibrational modes and Mo–O bond stretching frequencies. Changes in peak intensity and width further reveal doping-induced structural effects, with peak broadening suggesting increased lattice disorder or strain, and intensity variations reflecting changes in bond polarizability.

2.4.3.3 *UV-Visible-NIR Absorption Spectroscopy:*

UV-Vis absorption spectroscopy is essential for characterizing the electronic structure and optical properties of materials, providing insights into their absorption and bandgap. It is widely applied in fields such as chemistry, biochemistry, and materials science for both qualitative and quantitative analysis. Key applications include monitoring chemical reactions, determining concentrations, and optimizing materials for energy-efficient technologies [7]. The Beer-Lambert law states that a material's light absorption is directly proportional to its concentration and the optical path length. This relationship is mathematically expressed as:

$$A = \log_{10}\left(\frac{I}{I_0}\right) = \varepsilon \times c \times l \quad \ldots (2.3)$$

Where A is absorbance, ε is the absorptive coefficient, c is concentration, l is path length, and I_0 and I are the incident and transmitted light intensities, respectively.

The UV-Vis-NIR absorption spectra of the phosphor materials were recorded in the 200-800 nm wavelength range using a JASCO V770 spectrophotometer. The instrument utilizes a deuterium (D_2) lamp for UV light source and a tungsten lamp for the visible and NIR regions source. Detection is achieved using either a charge-coupled device (CCD) or a photomultiplier tube (PMT). The powdered sample, dispersed in ethanol, was placed in a quartz cuvette for analysis. The spectrophotometer's monochromator generates monochromatic light, which is split into two beams: one passes through the sample, and the other serves as a reference. The absorption characteristics are determined by comparing the two beams, with detection by the CCD or PMT. A ray diagram of this setup is shown in Fig. 2.9 (a), and the spectrophotometer is depicted in Fig. 2.9 (b).

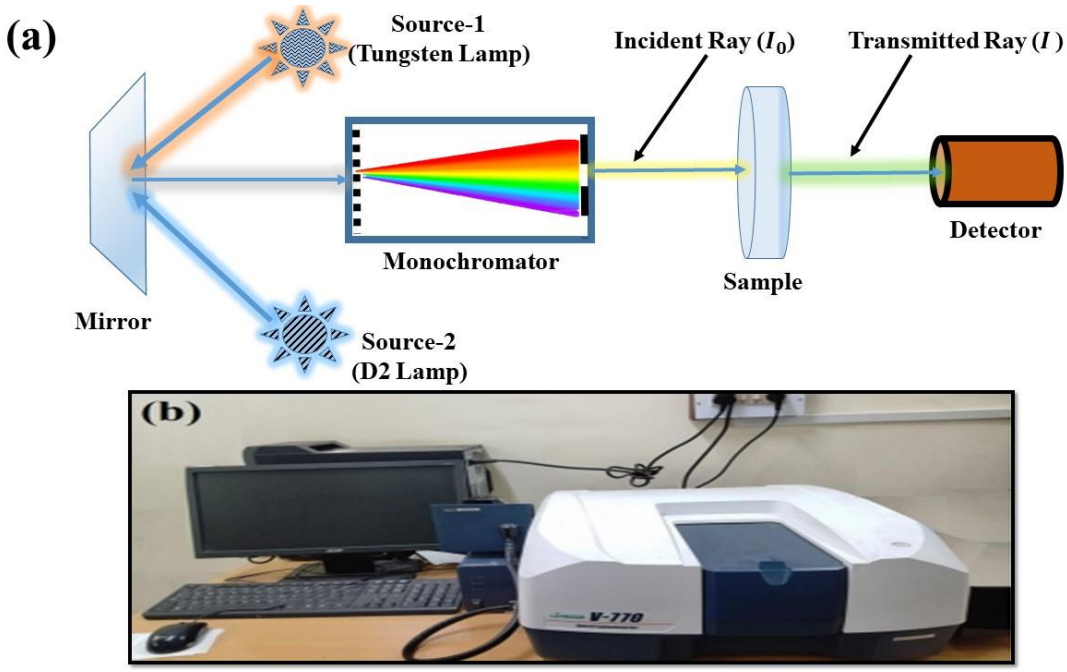

Figure 2.9 ***(a)*** *Ray-diagram of the UV-visible absorption analysis.* ***(b)*** *Digital photograph of JASCO V770 UV-Visible spectrophotometer (Department of Physics, IIT BHU).*

In this thesis, the optical bandgap of both pristine and Ln-doped $CaMoO_4$ phosphors was determined by analysing the absorption edge using the Tauc plot, represented by the equation

$$(\alpha h\nu)^{\frac{1}{n}} = A(h\nu - E_g) \ldots (2.4)$$

where E_g is the optical bandgap, α is the absorption coefficient, A is a constant, and hν is the incident photon energy. Mode of transition is determined by the '1/n'. For the direct allowed it is 1/2, and for direct forbidden it is 2/3. The '1/n' value for the indirect allowed and indirect forbidden is 2 and 3, respectively. The absorption bands observed in the spectra correspond to electronic transitions within the host and the lanthanide dopants, providing valuable insights into their energy levels and electronic structure.

2.4.3.4 *Photoluminescence (PL) Spectroscopy:*

Photoluminescence (PL) spectroscopy is a non-destructive, highly effective optical method for studying radiative transitions in materials. It offers valuable insights into the electronic structure and optical properties of phosphors, whether in solid or liquid form. When a sample is excited with photons of a specific energy, electrons are excited to higher energy states (a process known as photoexcitation). As these excited electrons return to lower energy levels, they release photons. The characteristics of the emitted light, including intensity, wavelength, and lifetime, among others, offer essential information about the material's optical properties and behaviour. PL spectroscopy is vital for analysing luminescent materials, as it enables the study of both photoluminescence excitation (PLE) and photoluminescence emission (PL) spectra. The PLE spectrum reveals the transitions from the ground state to excited states, while the PL spectrum provides insight into transitions from excited states to the ground state.

PL measurements were conducted using a Horiba Fluorolog-3 fluorescence spectrophotometer, depicted in Fig. 2.10(b), which uses a 450 W xenon lamp as the excitation source. This setup includes essential components such as monochromators and a photomultiplier tube (PMT) detector. The excitation monochromator selects specific wavelengths from the xenon lamp to excite the sample, while the emitted photons pass through the emission monochromator, which filters the light before it reaches the PMT detector. The PMT amplifies weak signals through a series of dynodes, ensuring accurate detection of the emitted light. The sample is positioned in a 90º geometry relative to the detector to minimize scattered light. To obtain the Photoluminescence Excitation (PLE) spectrum, the emission wavelength was held constant while the excitation wavelengths were scanned at progressively higher values. For the emission spectra, the excitation wavelength was fixed, and the emitted light was monitored over a range below the excitation wavelength. This experimental setup enabled the investigation of absorption transitions of ions and provided insights into the optical properties of the material, such as its bandgap, purity, and composition. Ray diagram consisting of main components is shown in Fig. 2.10 (a) illustrating the pathway of light from the excitation source through the monochromators and onto the detector. In this study, these spectra were recorded to assess the luminescent properties of lanthanide-doped $CaMoO_4$ phosphors, with a particular focus on the variations in emission intensities and wavelengths associated with different dopants, including Er^{3+}, Yb^{3+}, Tm^{3+}, and Ho^{3+}.

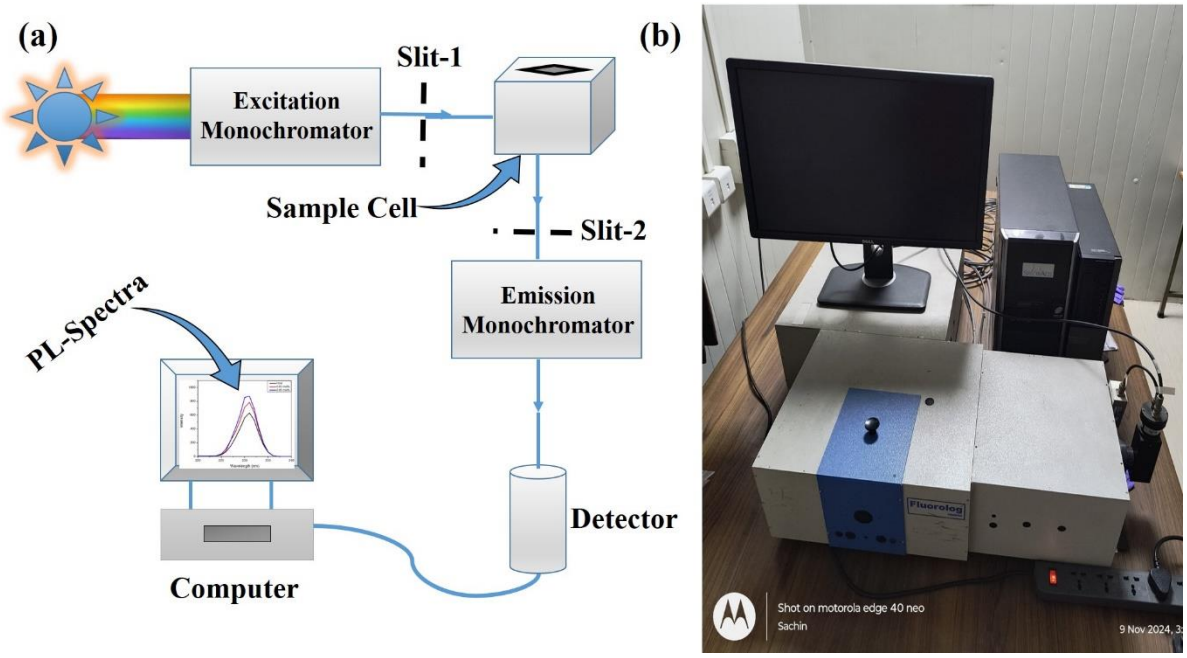

Figure 2.10 (a) A schematic of the PL spectrophotometer setup. (b) Digital photograph of Horiba Fluorolog-3 spectrophotometer (Department of Physics, IIT BHU).

2.4.3.5 *Upconversion Spectroscopy:*

Upconversion (UC) refers to the process by which lower-energy photons are absorbed and subsequently converted into higher-energy photons, which is a key phenomenon in lanthanide-based upconvertive phosphor materials. The relevance of upconversion lies in its unique ability to harness low-energy infrared (IR) photons, which are abundant in many practical applications, and convert them into visible or ultraviolet light. This capability is highly sought after for applications in areas such as bioimaging, solar energy harvesting, lighting, and display technologies. Lanthanide-based phosphors, especially those doped with ions like Er^{3+}, Tm^{3+}, or Ho^{3+}, exhibit strong upconversion properties due to their unique electronic structure and energy levels. The trivalent lanthanide ions have well-defined, long-lived excited states, which allow them to efficiently absorb multiple photons and emit light at higher energy levels. The mechanism behind upconversion in these materials typically involves multi-photon absorption, where two or more low-energy photons are absorbed sequentially by the lanthanide ions and then combined to emit a single higher-energy photon.

In the case of excitation at 980 nm, a common near-infrared (NIR) excitation wavelength, the energy of the incident photons is absorbed by the lanthanide ions and promoted to an excited state. This energy can be further transferred among the ions through cross-relaxation or other mechanisms, ultimately leading to the emission of visible light, such as green or red, depending on the specific dopant ions and the resulting electronic transitions. The measurement of upconversion typically involves monitoring the emitted light under NIR excitation and analysing the intensity, spectral features, and decay characteristics of the emitted photons.

In comparison to photoluminescence (PL), upconversion differs fundamentally in that it involves the absorption of multiple low-energy photons to produce a higher-energy photon, whereas PL is a simpler process where a material absorbs a single photon, excites an electron to a higher energy state, and then re-emits a lower-energy photon. The key difference is the number of photons involved and the wavelength range of both the absorbed and emitted light. While PL is useful for imaging and detecting materials, upconversion provides enhanced control over emission wavelengths, which is crucial for specific applications like bioimaging or solid-state lighting. Additionally, the ability of upconversion to operate in the NIR region makes it more compatible with biological tissues and optical fibers, giving it an edge over traditional PL for certain advanced technologies.

2.4.3.6 *Time Resolved Photoluminescence (TRPL) Spectroscopy*

Time-Resolved Photoluminescence (TRPL) studies are crucial for understanding the dynamics of excited states in luminescent materials [10]. By analysing the fluorescence decay profiles, TRPL provides insights into the lifetimes of excited states, which directly influence the material's efficiency and emission characteristics. This technique helps identify the role

of dopants and defects, optimize luminescent behaviour, and enhance phosphor performance by studying carrier recombination, energy transfer, and non-radiative decay mechanisms, making TRPL an indispensable tool for designing advanced phosphor materials with tailored optical properties.

In Time-Resolved Photoluminescence (TRPL), a short laser pulse excites the sample, and the emitted light intensity is measured as a function of time. The decay profile is typically modelled by a single exponential decay:

$$I(t) = I_0 e^{-\frac{t}{\tau}} \quad \ldots (2.6)$$

where I(t) is the photoluminescence (PL) intensity at time I_o is the initial intensity, and τ is the decay time or lifetime of the excited state. In addition to the single exponential function, the presence of double or triple lifetimes in inorganic phosphors is particularly significant, as it offers a deeper understanding of the complexity of the energy transfer process. Multiple decay components typically arise from different energy transfer mechanisms, such as radiative recombination, non-radiative decay, and energy trapping in defects or impurities. In many doped phosphors, the faster decay component is often associated with non-radiative processes like trap-assisted recombination, while the slower component corresponds to radiative recombination of free charge carriers or energy transfer between different dopant ions. The presence of multiple lifetimes can indicate the interaction between different excited states, such as those involving different levels of the dopant or host material, and can also reflect the heterogeneity of the local environment around the dopants. For instance, in materials exhibiting a double exponential decay, the PL intensity may follow a biexponential decay model:

$$I(t) = \sum_i A_i \, e^{-\frac{t}{\tau_i}} \quad \ldots (2.7)$$

The average decay time τ_{av} in the biexponential fit is expressed as

$$\tau_{av} = \frac{A_1\tau_1^2 + A_2\tau_2^2}{A_1\tau_1 + A_2\tau_2} \quad \ldots (2.8)$$

τ_1 represents the fast decay associated with trap-assisted nonradiative recombination, while τ_2 represents the slower decay related to the free charge carriers' radiative recombination. A_i is the decay amplitude for the decay τ_i. In the present thesis, the decay analysis has been performed by using 25W Xenon pulsed lamped which ***is*** attached to fluorolog-3 spectrometer (Model: FL3-11, Horiba Jobin Yvon Edison, MJ, USA).

2.5 Software Relevance in Scientific Research and Analysis

In modern scientific research, the use of specialized software has become indispensable for data analysis, visualization, and interpretation. Various software tools are designed to cater to specific types of data and experiments, enhancing both the accuracy and efficiency of research outcomes. This section discusses the relevance of several key software programs commonly used in this thesis, including *Fullprof Suite*, *ImageJ*, *Origin*, and *Colour Calculator v7.77*. These programs enhance the precision, efficiency, and depth of analysis in various areas of study, from crystallography and imaging to data visualization and spectral analysis.

2.5.1 Fullprof Suite for XRD Analysis

The *Fullprof Suite* is an essential software package for analysing X-ray diffraction (XRD) data. XRD is a powerful technique used to characterize the crystal structure of materials, and *Fullprof Suite* is specifically designed to perform detailed Rietveld refinements and structural

analysis. It is widely utilized in material science for determining crystal symmetry, lattice parameters, and atomic positions. The software offers robust tools for peak fitting, background subtraction, and refinement of diffraction patterns, allowing researchers to extract precise structural information from their XRD data. By automating the fitting process and providing a user-friendly interface, *Fullprof Suite* significantly reduces the time and complexity of data interpretation, making it an indispensable tool for crystallographers and materials scientists.

2.5.2 ImageJ for TEM and Image Processing

ImageJ is a versatile and widely used software for processing and analyzing scientific images, especially in the context of Transmission Electron Microscopy (TEM) and other imaging techniques. TEM is crucial for obtaining high-resolution images of nanoscale structures, and *ImageJ* provides a wide array of functions for image enhancement, particle analysis, and quantification. Researchers often use *ImageJ* to measure grain sizes, particle distributions, and surface morphologies in TEM images. The software supports various plug-ins, allowing for customization and the integration of new algorithms, which makes it particularly valuable for specialized analyses. Furthermore, its open-source nature ensures that it remains accessible to researchers, while its extensive user community continues to enhance its capabilities. As imaging becomes more central to material characterization, *ImageJ* serves as a vital tool for extracting quantitative information from visual data.

2.5.3 Origin Pro 2021

Origin is a comprehensive software suite designed for data analysis, graphing, and visualization. It is widely used for creating high-quality 2D and 3D plots, making it an essential tool for researchers who need to visualize complex experimental results. *Origin*

offers a range of customizable plotting options, including line graphs, scatter plots, contour plots, and surface plots, making it suitable for a variety of scientific applications. The software's powerful data analysis capabilities, such as curve fitting, statistical analysis, and peak deconvolution, allow researchers to gain deeper insights from their data. Whether used in experimental physics, chemistry, or biology, *Origin* is valuable for presenting results in a clear and professional manner, aiding in the communication of findings to both the scientific community and the broader public.

2.5.4 Colour Calculator v7.77 for Spectrum Colour Calculation

The *Colour Calculator v7.77* is a specialized tool used for calculating the colour coordinates of spectra, an essential function in fields like optics, materials science, and lighting research. By inputting spectral data, the software can determine various colour properties such as hue, saturation, brightness, and other colour metrics in both the RGB and CIE colour spaces. This is particularly useful for researchers studying the optical properties of materials, such as their absorption or emission spectra. The tool's ability to convert spectral data into precise colour values helps researchers to better understand the visual and photometric characteristics of their samples, which is critical in applications ranging from the design of optical devices to the analysis of light-emitting materials.